

UC Irvine

UC Irvine Previously Published Works

Title

Diffuse optical spectroscopy of melanoma-simulating silicone phantoms

Permalink

<https://escholarship.org/uc/item/21q103b0>

ISBN

9780819474339

Authors

Grant, Alexander M
Sry, Kelly
Saager, Rolf
et al.

Publication Date

2009-02-12

DOI

10.1117/12.809488

Copyright Information

This work is made available under the terms of a Creative Commons Attribution License, available at <https://creativecommons.org/licenses/by/4.0/>

Peer reviewed

Diffuse Optical Spectroscopy of Melanoma-Simulating Silicone Phantoms

Alexander M. Grant¹, Kelly Sry¹, Rolf Saager¹, Frederick Ayers¹, T. Joshua Pfefer², Kristen M. Kelly¹, Sheng-Hao Tseng¹, Anthony J. Durkin¹

¹Beckman Laser Institute, University of California, Irvine, CA 92617

²Food and Drug Administration, Silver Spring, MD 20993

ABSTRACT

Currently the only method for positively identifying malignant melanoma involves invasive and often undesirable biopsy procedures. Available *ex-vivo* data indicates increased vascularization in the lower regions of excised melanoma, as compared to dysplastic nevi. The ability to interrogate this region of tissue *in-vivo* could lead to useful diagnostic information. Using a newly developed fiber based superficial probe in conjunction with a steady-state frequency-domain photon migration (SSFDPM) system, we can probe the upper 1-2 mm of tissue, extracting functional information in the near infrared (650-1000 nm) range. To test the resolution and detection range of the superficial probe in this context, deformable silicone phantoms have been fabricated that simulate normal skin with melanocytic lesions. These phantoms consist of a two-layered matrix with the optical properties of normal light skin, containing several cylindrical inclusions that simulate highly absorbing pigmented lesions such as melanoma. These inclusions are varied in depth, diameter, and optical properties in order to fully test the probe's detection capabilities. It was found that, depending on absorption, we can typically probe to a depth of 1.0-1.5 mm in an inclusion, likely reaching the site of angiogenesis in an early-stage melanoma. Additionally, we can successfully interrogate normal tissue below lesions 1.5mm deep when absorption is about 0.4/mm or less. This data indicates that the superficial probe shows great promise for non-invasive diagnosis of pigmented lesions.

Keywords: biophotonics, diffuse optical spectroscopy, skin cancer, melanoma, tissue optical properties, tissue phantoms, Monte Carlo, handheld probe

1. INTRODUCTION

1.1. Melanoma

Skin cancer is now the most common form of cancer in the United States, where incidence of malignant melanoma is increasing faster than any other type of cancer¹. Melanoma is the deadliest form of skin cancer, and unfortunately is now responsible for over 80% of all skin cancer deaths². Since the prognosis is typically good with early diagnosis, the ability to deploy appropriate screening and early detection techniques on a widespread basis is essential. Unfortunately, even expert clinicians with many years of training have difficulty in differentiating cutaneous melanoma from benign look-alike lesions (benign melanocytic nevi; refer to Fig. 1 for examples of pigmented nevi). Although there are no conclusive data available indicating how many true melanomas are missed by physicians, there are data indicating that, depending on a physician's training, it takes from 5 to 100 benign lesion biopsies to find a single melanoma. Clearly, this process is not ideal; when dealing with potentially deadly cancers in a time-sensitive context, an accurate and efficient detection method is needed. New procedures utilizing the latest in bioengineering technology show great potential in this field³. Optical techniques such as diffuse optical spectroscopy (DOS) promise a fast and noninvasive way to quantify tissue composition and function *in-vivo*^{4,5}.

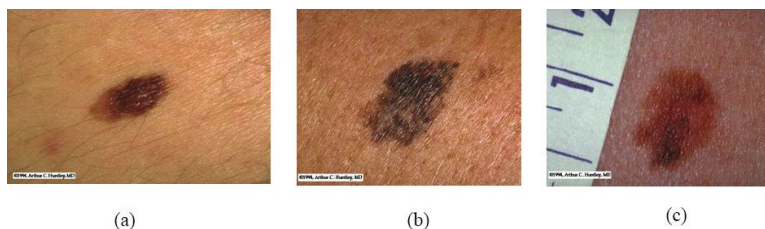


Figure 1. Pigmented lesions: (a) Dysplastic nevus. (b) Lentigo maligna melanoma. (c) Superficial spreading melanoma. (a) is a benign mole, while (b) and (c) are melanoma.

1.2. Diffuse optical spectroscopy

DOS uses interrogation with near-infrared light coupled with mathematical photon transport models to accurately determine optical absorption (μ_a) and reduced scattering (μ_s') properties of tissues. These properties in turn can be used to deduce physiologic functional information, such as water and lipid concentration and blood oxygen saturation of bulk biological tissues^{6,7}. Diffusion-based methods have, until recently, proven to be inadequate for quantitative studies of superficial tissues, as the standard models break down at this limit. However, Durkin et. al. have recently developed a new optical probe design and modeling approach that, when used in combination with a Steady-State Frequency-Domain Photon Migration (SSFDPM) platform (Fig. 2), can recover quantitative data on the optical and physiological properties of tissues at depths of less than 1mm⁸. The ability to recover data at this superficial depth is important because it is the relevant domain for the characterization of cutaneous melanoma and benign melanocytic nevi.

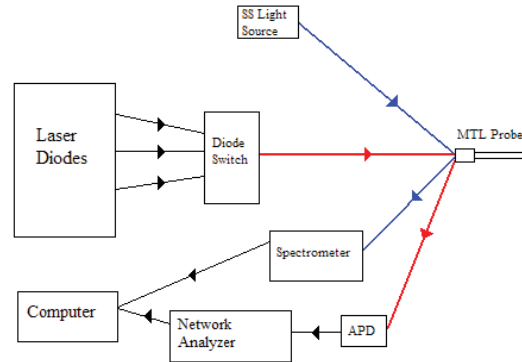


Figure 2. SSFDPM Setup – consists of both steady-state (SS) and frequency-domain (FDPM) elements. SS: white light source provides light for interrogation of tissue (through MTL probe), which is then reflected to the spectrometer. FDPM: laser diodes (through switching mechanism) provide light, which is reflected to avalanche photodiode (APD). Electrical signals are then sent to the network analyzer. The spectrometer and network analyzer interface with the computer running the data collection program.

1.3. Theory

SSFDPM measurements are taken in the *frequency domain*; laser light of certain wavelengths incident on the tissue is intensity-modulated at various frequencies in the RF range (typically 50-300 MHz). Light in the tissue experiences amplitude attenuation as a result of absorption, and modulation phase lag as a result of elastic scattering events (Rayleigh or Mie scattering depending on particle size). At each modulation frequency, the diffuse reflectance is collected from the tissue and its characteristic change in phase and amplitude is used in conjunction with a radiation transport model to calculate the optical properties of the tissue in the form of the absorption (μ_a) and reduced scattering (μ_s') coefficients. The absorption coefficient represents the probability that a photon will be absorbed within a certain path length. The reduced scattering coefficient corresponds to the probability of forward isotropic scattering within a certain path length, and is defined as $\mu_s' = \mu_s(1-g)$ where g is the anisotropy coefficient of the tissue ($g = \langle \cos(\theta) \rangle$ where θ is the angle of scattering deflection; typical biological tissues: $0.65 < g < 0.95$). Diffuse reflectance data collected from a steady-state white light source is fit to the values calculated from the laser diodes to provide a full spectrum of optical properties in the wavelength range of 650-1000 nm⁴.

In radiation transport theory, rather than treating light propagation in tissue from an electromagnetic wave interaction point of view, light is modeled as discrete photons that undergo absorption or scattering due to the biological structure and composition of the tissue. In this somewhat simplified model, effects such as polarization, interference, and diffraction are not considered. The *radiative transfer equation* that forms the basis of this approach is

$$\frac{\partial L(\vec{r}, \hat{s}, t) / c}{\partial t} = -\hat{s} \cdot \nabla L(\vec{r}, \hat{s}, t) - (\mu_a + \mu_s) L(\vec{r}, \hat{s}, t) + \mu_s \int_{4\pi} L(\vec{r}, \hat{s}', t) P(\hat{s}' \cdot \hat{s}) d\Omega' + S(\vec{r}, \hat{s}, t) \quad (1)$$

where L is the radiance, c is the speed of light, μ_a and μ_s are the absorption and scattering coefficients respectively, P is the normalized phase function, \hat{s} is a unit vector pointing in the direction of photon propagation and S represents the source. In the regime where $\mu_s' \gg \mu_a$ (as is the case with many biological tissues of interest), this equation can be greatly simplified in what is known as the diffusion approximation. The resulting *diffusion equation* is:

$$\frac{\partial \Phi(\vec{r}, t) / c}{\partial t} + \mu_a \Phi(\vec{r}, t) - D \nabla^2 \Phi(\vec{r}, t) = S(\vec{r}, t) \quad (2)$$

where $D = \frac{1}{3(\mu_a + \mu_s')}$ and Φ is the fluence rate. The diffusion approximation to the radiative transfer equation is

used to recover optical properties from DOS measurements taken with the SSFDPM instrument (the specifics of this approach will not be discussed here; for a detailed treatment see^{4,9}).

In a typical DOS measurement of a thick tissue such as breast, a probe source-detector geometry similar to that illustrated in Fig. 3(a) is used. The average depth of interrogation is between 1 and 2 cm. With this setup, the assumptions inherent in the standard modeling approach are satisfied. That is, photons absorbed in the tissue have undergone a sufficient number of scattering events for the diffusion approximation to apply, and boundary effects are negligible; thus, optical properties can be recovered accurately. Interrogation depth is typically proportional to source-detector separation, so to probe superficial tissues we must have a short source-detector separation (~3mm). At this short separation, though, photon path lengths are not large enough for the diffusion approximation to apply. Because more than 80% of all cancers originate in tissue volumes that are 1mm or less below the tissue surface, diffusion based methods have proven ineffective for applications such as skin cancer studies¹⁰. The aforementioned new probe design uses a modified two-layer (MTL) diffusion geometry in which a high scattering ($\mu_s' = 45/\text{mm}$ @ 660nm), low absorption ($\mu_a = 10^{-7}/\text{mm}$) layer is placed on the surface of the sample and below the source fiber, as depicted in Fig. 3(b). In this geometry the detection fiber passes through the scattering layer and is in direct contact with the surface of the tissue. This configuration increases scattering events and effective photon path lengths, enabling the use of a modified two-layer diffusion model in order to accurately predict the optical properties of superficial tissue volumes of interest¹¹. Clinical studies of normal tissue measured with the superficial probe have shown excellent agreement with *ex-vivo* skin data published by Simpson et. al. (Fig. 4), and testing has indicated that it can be used to accurately measure optical properties over a wide range of absorption and scattering coefficients ($\mu_a \approx 0.05\text{-}0.4/\text{mm}$ and $\mu_s' \approx 0.5\text{-}2.5/\text{mm}$)^{12,13}.

The ultimate goal of the research oriented around this probe is to facilitate investigation that will characterize tumor optical properties with the hopes of developing the means to non-invasively distinguish malignant from benign lesions. In this study we aim to determine how both the dimensions of a lesion and the surrounding tissue affect measurement with the superficial probe. This requires successful detection of minute changes in optical properties at the surface of skin. Thus far, the performance of the superficial probe has been only assessed in semi-infinite, homogeneous phantoms; it is therefore necessary to conduct an additional set of studies to simulate the heterogeneity that may typify one or more properties of an *in-vivo* melanocytic lesion. Solid phantoms can be constructed in which the absorption and scattering coefficients can be precisely controlled and chromophore (biological compounds that absorb and reflect light) concentrations can be predetermined depending on which spectral regions are of particular interest¹⁴.

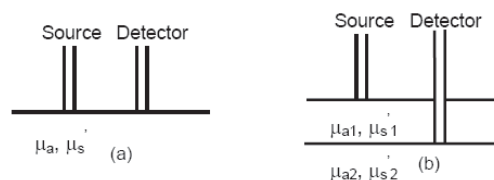


Figure 3. (a) Typical DOS measurement geometry (b) Modified two-layer (MTL) geometry. The top layer in (b) is a high scattering and low absorption medium (Spectralon).

1.4. Melanoma-simulating phantoms

Layered skin-simulating phantoms were constructed that contained heterogeneities with increased absorption relative to the surrounding homogenous tissue-simulating matrix, and their properties were measured with the superficial probe. During this study a method for the construction of phantoms having areas of increased pigment that vary in depth and thickness was repeatedly utilized and refined. Working from extensive prior experience using the superficial probe with the SSFDPM setup, a reproducible experimental method for measuring each phantom's properties in various ways, which would test the practical resolution of the probe, was designed. Monte Carlo simulations were also carried out and analyzed to determine how light was being distributed in the simulated lesions. Based on these simulations, we generally

expected that if light was reaching two distinct layers of a phantom (or tissue), the recovered optical property values would fall somewhere between those of each layer and would depend on the thickness of the upper layer (assuming semi-infinite lower layer).

This strategy for characterization of heterogeneous phantoms as interrogated via the superficial probe has provided a means for developing a coherent understanding of optical signals acquired with the probe. In particular, we have elucidated some of its capabilities, including identifying which optical properties we can measure reliably and the size limitations on melanocytic lesions we can successfully interrogate. This information will be valuable for making measurements and analyzing data in actual human tissue studies (a current phase of the research).

2. EXPERIMENTAL DESIGN AND METHOD

Solid phantoms were fabricated that consisted primarily of the silicone rubber PDMS [poly(dimethyl siloxane)], which provided the matrix of chromophore suspension. This material allowed for the creation of somewhat deformable solid phantoms that were reusable and stable over time. Deformability is a desirable property that better simulates the optical/physical probe/sample contact that is encountered with skin (as opposed to epoxy-based phantoms, which are non-deformable and result in poor contact). The absorber used was India ink, and TiO_2 was the scatterer. The phantoms consisted of two distinct layers. The substrate or “subcutaneous” layer was approximately 2cm thick and had relatively low absorption and high scattering ($\mu_a = 0.03/\text{mm}$, $\mu_s' = 3.00/\text{mm}$ @660nm). This layer was first poured into the phantom mold and cured for 24 hours, after which time the second layer, or “dermis,” was poured on top and cured, again for 24 hours. This upper dermis layer was 3mm thick in order to approximate the thickness of human dermis on the upper back. It was more highly absorbing and less scattering than the subcutaneous layer, in order to mimic the optical properties of the upper melanized layers of Caucasian skin ($\mu_a = 0.05/\text{mm}$, $\mu_s' = 2.45/\text{mm}$ @660nm). Based on previous tests conducted with the superficial diffusing probe, it was expected that light would likely not reach beyond 1-2mm in these phantoms; since the dermis layer was 3mm thick, it was assumed that the interface of the two silicone layers would not be probed to any significant extent so that only interactions involving the dermis and the inclusions needed to be considered. Four cylindrical cavities were created in the top layer of each phantom by insertion of Delrin rods into the silicone during the curing process. These rods were held in the desired position and at the correct depths by a clamping fixture above the phantom mold, and were removed when the silicone was fully cured. The final step was to fill in each cavity with a highly absorbing material to simulate a melanoma in each location. For the cases in which the simulated melanomas were silicone-based, the target optical properties were chosen to correspond approximately to African skin measured in clinical studies ($\mu_a = 0.4/\text{mm}$, $\mu_s' = 2.00/\text{mm}$ @660nm). This set of optical properties was chosen for the simulated melanoma inclusions because conclusive published data on melanoma optical properties have been, up until now, unavailable. The chosen optical properties ultimately corresponded well with those of lesions measured *in-vivo* in the clinical study, which will be described later.

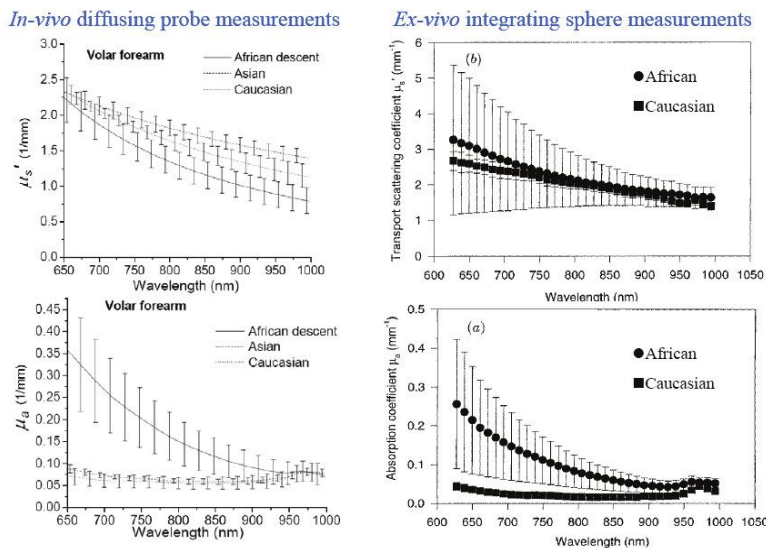


Figure 4. Plots on the left represent *in-vivo* optical properties collected from the volar forearms of 15 volunteers (5 of each skin type) using the superficial diffusing probe. Plots on the right represent similar skin optical properties collected *ex-vivo* by Simpson et. al.

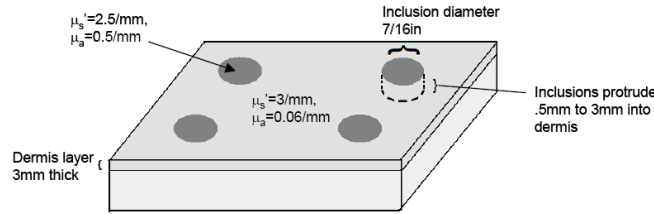


Figure 5. Diagram of melanoma-simulating phantom features.

Three main variations on this simulated melanoma design were constructed. In the first, both the depth and the diameter of the inclusion were varied (melanomas were silicone-based and all of the same optical properties). This phantom was intended to determine the effects of the dermis-melanoma interface on probe readings as the lateral edge of the inclusion approached the area of interrogation. In the second variation, the diameter of the inclusion was constant, and the depth was varied. Again, the inclusions were silicone and all had the same optical properties. This phantom was meant to provide insight into the actual tissue depth probed in a melanoma measurement. The third variation contained inclusions of constant diameter and depth but varied optical properties. Silicone was not used to simulate melanomas; instead, gelatin-based phantoms of varying absorption were placed in the cavities so that the sensitivity of the probe could be tested with regards to range and precision. This phantom gave insight into how much the underlying dermis tissue contributed to recovered optical properties in intermediate-size melanomas relative to their actual properties. The general phantom geometry is represented in Fig. 5.

Typically, the measurement process consisted of placement of the probe directly on top center of a melanoma inclusion, orthogonal to the upper phantom surface. Most measurements took about 90 seconds to complete. As such, the probe was held in place above the phantom with a clamp to guarantee that the measurement was not affected by unnecessary motion. In the case of the diameter and depth varied melanoma phantom, some of the inclusions were of smaller diameter than the probe tip; the melanomas were centered by eye below the probe tip, as they were typically still large enough to cover the 3mm source-detector separation of the probe. Measurements were also taken on a sample of the bulk phantom material used to make the melanomas for each phantom; each of these bulk samples was several centimeters thick, effectively serving as a semi-infinite slab of reference material. This bulk material (silicone or gelatin) measurement functioned as a control group, allowing the shift in optical properties resulting from inclusion in the surrounding dermis to be determined. As the SSFDPM system requires a calibration standard to correct for erroneous instrument response introduced into the data, several tissue phantoms of known optical properties were measured as well. These phantoms ranged from low absorption for the surrounding dermis to relatively high absorption for the melanomas, and included calibration phantoms having intermediate values of optical properties as well.

3. EXPERIMENTAL RESULTS

The first melanoma phantom (“diameter and depth varied”) contained inclusions of different diameters, 3/16in, 1/4in, 3/8in, and 7/16in, and depth in dermis of 0.5mm, 1mm, 2mm, and 3mm, respectively. Note that inclusion diameters are reported in the unit system provided by the makers of the Delrin rods (McMaster Carr); otherwise, dimensions here are generally reported in mm and cm. The rough proportionality of depth and diameter was meant to simulate different stages of lesion growth. It was discovered that adhesion of curing silicone to the Delrin rods caused a creeping upwards of the edges of the inclusion, which in this case resulted in inclusions that were raised out from the dermis layer and a few millimeters deeper than originally intended.

This extra thickness of highly absorbing material also likely resulted in almost no measurable light reaching below any of the inclusions (as will be illustrated in the results of Monte Carlo simulations that are presented for the second set of melanoma-simulating phantoms), which in this case is acceptable as the phantom was designed to test only for lateral edge effects. Since the inclusions were slightly raised out of the surrounding matrix, some of the probe’s Spectralon surface did not make contact with any part of the phantom, resulting in an air gap between the outer edge of the probe and the phantom. Such gaps are not accounted for in the photon migration model governing the probe’s performance. However, this gap on the smaller inclusions did not appear to adversely affect measurement or processing; Fig. 6 shows that recovered data from all four inclusions (m1-m4) and the bulk sample (dark blue line) have similar properties and shape, and do not by themselves suggest any anomalous behavior. This is likely because even the smaller inclusions were sufficiently large to cover the source-detector area of the probe when centered, and the air gap was not directly in the path of the photons traveling between them. It is clear from Fig. 6, however, that there is a significant drop in

absorption for each inclusion when compared to the bulk sample. The results of the depth-varied phantom experiment (to be discussed later) suggest that for inclusions of these particular optical properties, depth difference based on absorption readings is not discernible beyond 1mm thickness. Each of the inclusions in the diameter and depth varied phantom are thicker than 1mm (including raised section), so we conclude that the drop in absorption versus the bulk material is not related to inclusion depth. This consistent drop could be a result of the raised profile of the inclusions out of the phantom surface, but further testing is necessary to draw conclusions about the cause. Similar optical properties were recovered for all diameters of inclusions; however in some cases, as in Fig. 6, it was observed that inclusions of larger diameter were slightly more absorbing over much of the wavelength range, with a clearly discernible relation between diameter and absorption. Overall, these results suggest that typically, very little light travels beyond the area directly beneath the source and detector fibers in the center of the probe, but it may be enough to subtly affect absorption values in some cases. The equipment is often not sensitive enough to pick up these slight variations in signal, so we conclude that lesion diameter does not have a significant effect on recovered optical properties, given sufficient area to cover the probing surface. Future experimentation is needed to determine whether this conclusion holds for inclusions having lower absorption properties. In order to conclusively test the effects of inclusion diameter, as well as explain the absorption decrease from bulk values, it will in the future be necessary to construct a phantom with varying inclusion diameter and constant depth, as well as inclusions that are relatively flush with the dermis layer.

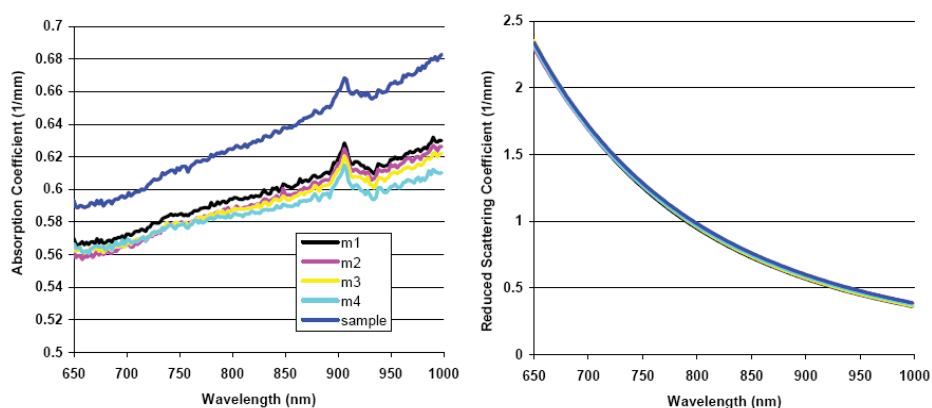


Figure 6. Optical properties of diameter and depth varied melanoma-simulating phantom. The largest inclusion is designated ‘m1’ while the smallest is ‘m4’.

The second variation of the melanoma phantom geometry (“depth-varied”) contained four inclusions, all of 7/16in diameter. These inclusions were of depth 0.5, 1, 2, and 3 mm, with relatively little surface protrusion. This larger diameter was chosen to eliminate any uncertainties regarding edge effects, since the entire probing surface fit easily within the diameter of the inclusions. To prevent the formation of raised inclusion edges such as those encountered in the first melanoma phantom, a scalpel was used to trim the silicone above the dermis before each Delrin rod was removed; as a result, the inclusions protrude very little from the dermis surface.

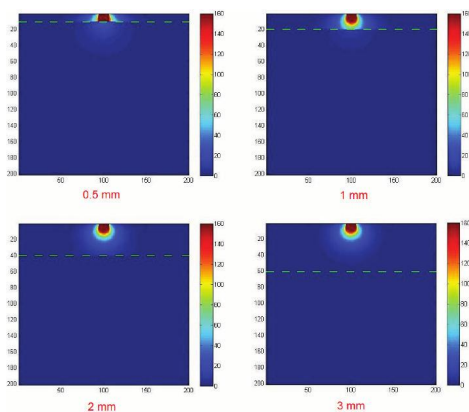


Figure 7. Results of Monte Carlo simulations (1cm^2) in which the top highly absorbing layer has been varied in thickness (separation between layers denoted by green dashed line). The plots represent energy deposition in J/cm^2 .

Monte Carlo photon extinction simulations were run based on this phantom geometry before it was tested experimentally. This series of Monte Carlo simulations utilizes a two-dimensional material grid wherein each voxel is assigned a number designating it as a certain type of tissue with specified optical properties such as absorption, scattering, anisotropy, and index of refraction¹⁵. Material grids of area 1cm² were designed with a high-absorbing “melanoma” layer on top of a lighter “dermis” layer that reached to the bottom of the grid (viewed as a vertical phantom cross-section). The top layer was varied in thickness to match the four inclusions in the depth-varied phantom. The optical properties roughly matched those of the multi-layer melanoma phantoms. The melanoma layer had $\mu_a = 0.4/\text{mm}$ and $\mu_s' = 2.0/\text{mm}$ while the dermis had $\mu_a = 0.06/\text{mm}$ and $\mu_s' = 3.0/\text{mm}$. Each simulation was run with 100,000 photons injected; the results are shown in Fig. 7. From the energy deposition density plots it is clear that as the dark upper layer becomes thicker, much more light energy is absorbed above the lower light layer. Since the amount of light entering the tissue volume is the same in any measurement, a thicker dark layer means that less of the light is actually entering the tissue below the inclusion. This is of great interest because the ability to probe the lower regions of a melanoma for vascularization changes is important for diagnosis^{2,16}. From these results we surmise that as a melanoma-simulating inclusion becomes thicker, the lighter tissue below will have a diminishing effect on the recovered optical properties of an inclusion measurement.

Measurements on each phantom inclusion revealed that light had very little penetration for inclusions of thickness 1mm or more, as illustrated in Fig. 8. From the results it is clear that the dermis layer is significantly sampled only in the 0.5mm inclusion; there is large drop in absorption, and a more slight increase in reduced scattering (pink lines in Fig. 8). Recovered optical properties were nearly identical for the other three melanomas (black, dark blue, and light blue lines on Fig. 8), and matched the properties of the bulk melanoma sample material (green lines on Fig. 8). These optical properties were found to be $\mu_a \approx 0.6/\text{mm}$ and $\mu_s' \approx 2.4/\text{mm}$ (somewhat different from the target values of $\mu_a \approx 0.4/\text{mm}$ and $\mu_s' \approx 2.0/\text{mm}$). These values clearly match the optical properties of the three deeper melanomas, suggesting that measurable light does not penetrate beyond the inclusions in these cases.

Since chromophore concentration fits based on superficial probe data will, in future *in-vivo* application of this technology, be calculated using absorption coefficient values, it is important for the probe to accurately resolve absolute values of and slight variations in absorption. As an initial trial, a series of Monte Carlo simulations were again conducted in order to develop some intuition for light distribution in real samples. As in the depth-varied experiment, 1cm² material property grids were constructed with a highly absorbing upper “melanoma” layer and lighter “dermis” tissue underneath. In this series of simulations, however, the top layer was of uniform 1mm thickness, and only its absorption coefficient was varied (between 0.1/mm and 0.6/mm in six steps); $\mu_s' = 1.5/\text{mm}$. The dermis layer had $\mu_a = 0.06/\text{mm}$ and $\mu_s' = 3.0/\text{mm}$. Each simulation was run with 100,000 photons injected. As is evident from the energy deposition plots (Fig. 9), varying absorption created an effect analogous to varying layer thickness. Namely, as the absorption coefficient is increased, the amount of light energy absorbed in the dark layer quickly increases, leaving less available to probe the dermis tissue. The simulation results led to the expectation that measurements on darker melanomas would show less evidence of the light lower tissue, as there would be less of a shift in their recovered optical properties.

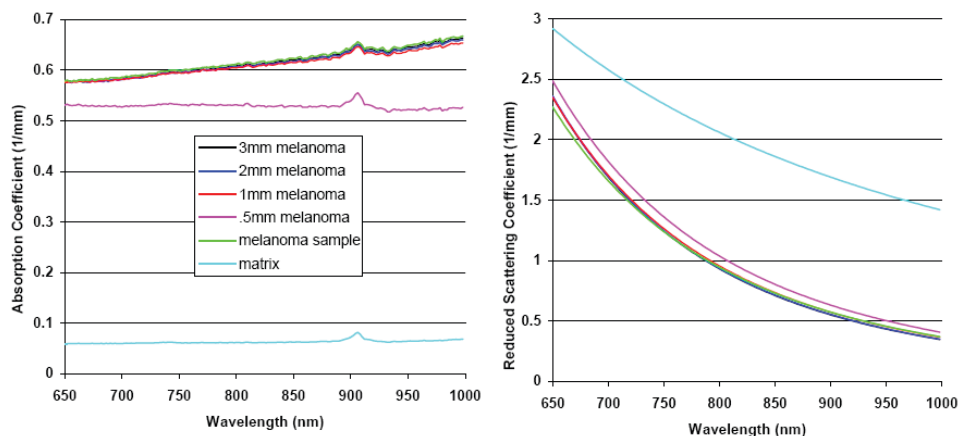


Figure 8. Optical properties of depth-varied melanoma-simulating phantom. ‘Matrix’ refers to the light “dermis” surrounding the inclusions.

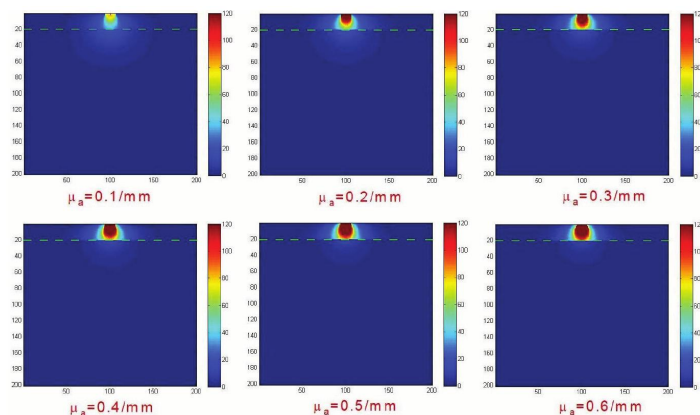


Figure 9. Results of Monte Carlo simulations. The top layer is a constant thickness of 1mm and has been varied only in absorption coefficient μ_a (separation between layers denoted by green dashed line). The plots represent energy deposition in J/cm^2 .

To perform the corresponding physical experiment (“absorption-varied”), inclusions of depth about 1.5mm were created in a two-layered phantom as before. This depth was chosen because it is typical of a melanoma that has not yet reached its final stages or metastasized, and based on the results of the depth-varied melanoma phantom it is likely that some light could still penetrate inclusions of this thickness, provided they are not too highly absorbing. The silicone melanomas of the previous phantoms are permanently bound to the silicone tissue matrix once they cure, and the creation of an all-silicone melanoma phantom takes several days, as each element needs to cure before the next one can be added. Because of these limitations, silicone is not a practical material for constructing many different multi-layer phantoms with different optical properties. Instead, gelatin was used as substrate for the melanomas in the third phantom iteration. Gelatin works well because phantoms can be prepared relatively quickly, and do not require lengthy curing or setting periods. Once the gelatin substrate was made, the appropriate amount of absorber (India ink) and scatterer (Intralipid) were added and the mixture was stirred. While still in a warm liquid form, the gelatin was poured into each of the four inclusions as before, and left for a few minutes to cool and partially solidify so that probe measurements could be made. Care was taken to ensure that each gelatin inclusion was poured to the same height in the phantom cavity, as surface tension would often allow the inclusion to extend upwards beyond the silicone border, and inconsistent depths could result. When a melanoma was no longer needed for measurement, it was simply peeled out of the silicone cavity and discarded. The amount of India ink was varied in each new gelatin phantom to create phantoms with absorption coefficients ranging from 0.15/mm to 0.65/mm. Scattering was kept relatively constant although some variation was observed, likely as a result of India ink molecules clustering in solution and contributing to elastic scattering of photons (Fig. 10).

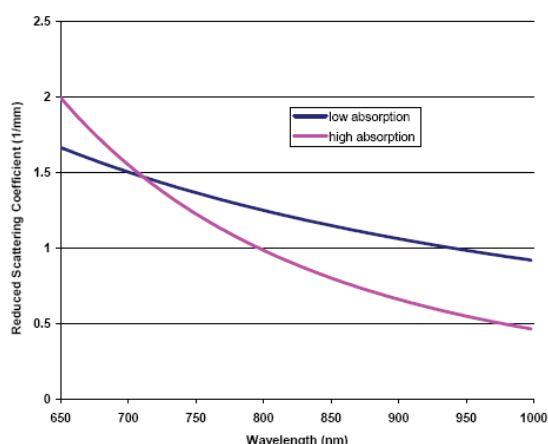


Figure 10. Plot of reduced scattering in two gelatin phantoms. “Low absorption” has $\mu_a = 0.15/mm$ and “high absorption” has $\mu_a = 0.65/mm$ @660nm. Both phantoms contain same amount of Intralipid (scatterer). Note the difference in curve shape, and below 700nm, the higher scattering for high absorbing phantom. This behavior could be a result of the clustering of India ink particles, affecting scattering. In principle the plots should be identical.

Occasionally the use of different calibration phantoms would yield conflicting optical property values for a single superficial probe measurement (this is due to instrument response not being constant for samples with different optical properties). A spectrophotometer (Shimadzu UV-3600) with integrating sphere attachment was utilized to determine the true optical properties of the gelatin phantoms. Reflectance and transmittance measurements were taken on thin slices of gelatin and optical properties were calculated using Prahl's inverse adding-doubling algorithm¹⁷. This method allowed us to determine which calibration phantom yielded the most accurate results for given sample; that phantom would then be used to calibrate subsequent probe measurements on the sample. Methods of deducing sample optical properties using an integrating sphere have been used successfully for many years. However, the necessity of using relatively thin samples limits its usefulness to mostly *ex-vivo* measurements and phantom validation; it has limited utility with respect to *in-vivo* tissue properties.

The results of this third set of melanoma-simulating phantoms are plotted in Fig. 11. In the lighter inclusions ($\mu_a < 0.4/\text{mm}$), recovered absorption (at 660nm) is typically 20-30% higher than in the bulk melanoma sample (the blue line represents bulk sample versus inclusion absorption), showing significant probing of the dermis. The data suggest that as the inclusion μ_a increases beyond about 0.4/mm, the dermis becomes either virtually undetectable or not consistently detectable (points are either close to the pink line or have large uncertainty). However, below μ_a of about 0.4/mm, the probe's ability to detect lighter tissue below a melanoma of this depth is excellent. Indeed, it is likely that this limiting absorption value would increase for thinner, earlier stage melanomas, enhancing the likelihood of detection even for darker lesions. The error bars in this plot represent the standard deviation of the measurements on four inclusions that are ostensibly the same. The large deviation apparent in two of the measurements could have resulted from inconsistencies in inclusion depth or subtleties in probe placement among trials.

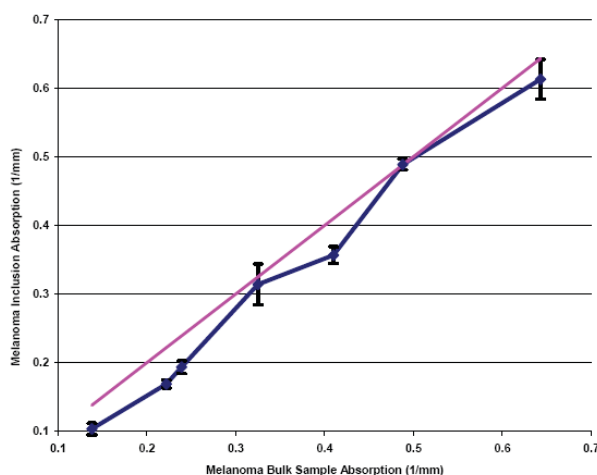


Figure 11. Absorption-varied melanoma-simulating phantom measurement results. The blue line represents the absorption coefficient (@660nm) of bulk “melanoma” material alone plotted against absorption of an inclusion (in dermis matrix) made with the same bulk material. Error bars represent standard deviation of measurements on four inclusions made with the same material. Pink line represents hypothetical case in which bulk melanoma sample and matrix inclusion melanoma are measured to have identical absorption for every value.

In particular, the irregularity in the trial at bulk sample $\mu_a = 0.325/\text{mm}$ could be due to the recurrence of a phenomenon observed by Tseng et. al. in which the photon diffusion processing algorithm generates optical property values inconsistent with the trend for layered phantoms with particular characteristics⁸. They found that at a 3mm source-detector separation (such as that used in our superficial probe) and with a top phantom layer 1mm thick, recovered absorption and scattering values sharply increased beyond benchmark predictions. It is possible that our particular combination of lesion thickness and optical properties has triggered a similar response in this case; more thorough investigation into this topic is necessary to draw any definite conclusions. Though from the data it is apparent that (at this depth) lighter tissue cannot be reliably probed to a significant extent at μ_a of about 0.5/mm and above, it is interesting to note that the absorption spectra of even the darker gelatin inclusions display at least some vestige of the characteristic silicone absorption peak at about 906nm (Fig. 12). This peak is absent in pure gelatin and more apparent in the lighter inclusions, supporting the hypothesis that more light reaches to the (silicone) dermis layer and back in these

cases. It was, however, observed in even the darkest inclusions tested, and is a definite indication that some dermis was still being probed despite the high absorption.

The observed drop in absorption due to probing of tissue under the lesion could potentially be used to make an estimate of the thickness of the lesion, though we have not yet collected enough data to observe a definite relationship between thickness and a characteristic absorption decrease. More phantom fabrication and experimentation is required to establish whether or not a model for such a determination is feasible; the next logical step in the melanoma phantom geometry is a phantom in which both inclusion depth and optical properties are varied. This would allow simultaneous tracking of multiple parameters and their effect on recovered optical properties, which would ideally lead to a set of known shifts in absorption for lesions of a specific depth, when compared to a normal tissue measurement.

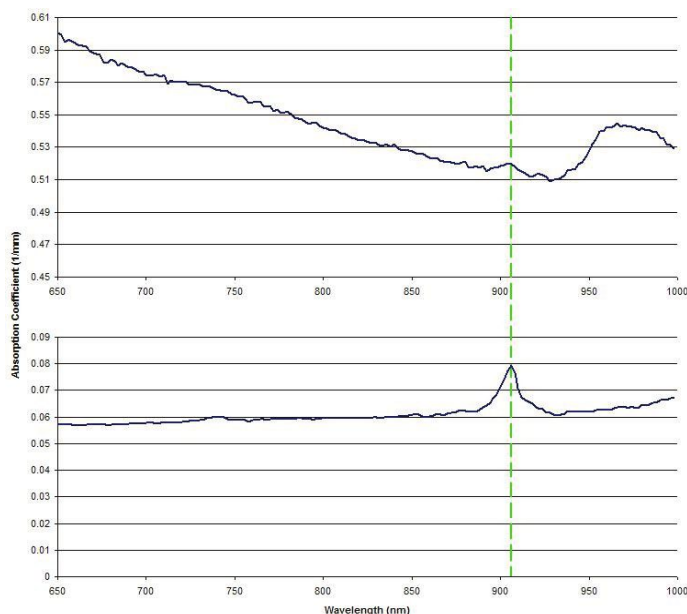


Figure 12. Representation of characteristic silicone absorption peak at ~906nm. Lower plot represents phantom dermis material only (silicone); the peak is clearly visible (marked with green line). Upper plot represents highly absorbing gelatin phantom inclusion in dermis; the silicone peak is still visible, though less pronounced than in the former case.

The diffusion approximation to the radiative transfer equation is only valid in cases where the reduced scattering coefficient is much greater than the absorption coefficient (typically two orders of magnitude). In the experiments described above, this difference is often less than one order of magnitude, leading to some questions as to the probe's reliability in this regime. For example, measurements were taken on a gelatin phantom with recovered optical properties of $\mu_a \approx 0.4/\text{mm}$ and $\mu_s' \approx 1.6/\text{mm}$ @660nm. In this case reduced scattering is only four times greater than absorption; clearly this is not an ideal application of the diffusion approximation, and the equipment would generally not be expected to yield accurate results. However, spectrophotometer integrating sphere measurements were in excellent agreement with probe values, indicating that the two-layer algorithm can be quite robust even when near the edge of model applicability. This result is encouraging, as both normal dark skin and pigmented lesions often have optical property values recovered in this range. A more sophisticated computational model for light propagation may be required as this technology progresses, though, to ensure accurate data regardless of optical properties since it is clear that the model breaks down in the case of very dark skin. Generally, scattering does not vary greatly among different ethnicities as it is related mostly to overall tissue structure, unlike absorption¹³. In clinical studies of very dark skin, superficial probe measurements have occasionally returned exceptionally high reduced scattering values ($\mu_s' \approx 5/\text{mm}$) coupled with absorption values that are likely somewhat lower than reality ($\mu_a \approx 0.2/\text{mm}$). It is believed that in such a case the processing algorithm has arrived at an incorrect conclusion, possibly by encountering a local minimum in the nonlinear least-squares fitting used to generate optical properties from the raw phase and amplitude data. This behavior may result when the true values cannot be modeled with diffusion theory.

4. PROBE REDESIGN

Clinical studies with the superficial probe have shown that highly absorbing tissues dramatically reduce the amount of light reflected back to the detector, leading to a decrease in the signal to noise ratio of the data recovered and inaccurate optical properties. It is inevitable that there is some amount of light leakage in any coupling between optical fibers, and the fiber optic multiplexer that acts as the intermediate between the laser diodes and the superficial probe introduces two additional fiber couplings into the system. A simple experiment was conducted to determine how much light is lost between the diode and the probe tip when it is passed through the multiplexer. A Newport Multi-Function Optical Meter (model 1835-C) was used with a Newport optical sensor (model 818-SL without attenuator) to detect the incident power of light emerging from the probe versus the light directly from the laser diode. It was found that the light intensity decreased by a factor of about three to five when passed through the multiplexer and probe together. In light of these results, revisions were made to the superficial diffusing probe design with the intention of eliminating the need for a multiplexer, thus decreasing light loss. To accomplish this, a new probe was fabricated in which the fibers connecting to the diodes were butt-coupled to the source fiber (design limitations allow for four diodes instead of six), so that the probe itself connects directly to the lasers. This design has several advantages over the previous version. Elimination of the multiplexer means less moving parts and equipment are necessary for operation. In addition, the probe can directly connect to other SSFDPM systems without the need to ensure software and hardware capability with the multiplexer. Initial results with the new probe are promising. To compare its light throughput with that of the previous design, the same Newport optical sensor was coupled to the detector fiber, and the probe tip was placed on a light tissue phantom while each laser diode was switched on. Fig. 13 shows that the new probe has increased throughput with all six laser diodes as compared with the previous design. The difference is especially dramatic in the higher wavelengths. For example, at 850nm, the laser throughput increased from 101nW to 274nW, a jump of 271%. We believe that this new design will allow us to more effectively interrogate dark tissue in clinical trials.

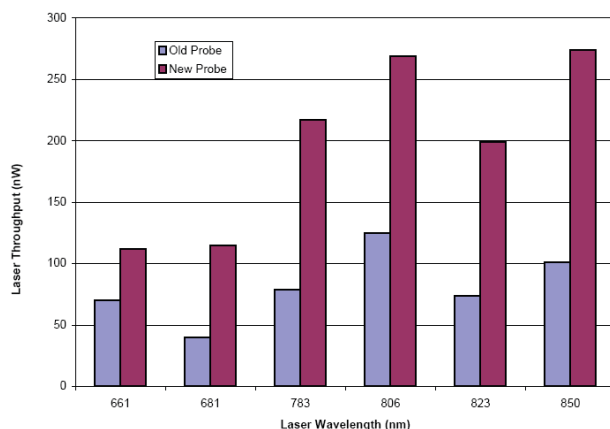


Figure 13. Comparison of laser power throughput of standard (old) and redesigned (new) probes.

5. CONCLUSIONS

We have successfully applied the superficial diffusing probe in a number of different scenarios, and have gained valuable knowledge about its abilities and potential. In this study we have made the first accurate optical property measurements of tissue phantoms containing inhomogeneities, the optical properties of which are consistent with those of *in-vivo* melanocytic lesions that we measured. By varying the phantoms' physical parameters we have determined that we cannot probe the dermis tissue below a lesion of about 1.0-1.5mm in thickness, depending on how highly absorbing it is. We have also learned that for a relatively thin lesion (~1.5mm), we cannot consistently probe dermis tissue if the absorption coefficient is beyond about 0.4/mm. These measurements also suggest that with further investigation, it may be possible to extrapolate lesion thickness from optical properties. Measurements on simulated lesions of different diameters have shown that this dimension does not have a great influence on recovered optical properties, suggesting that when clinical measurements are made, data related to vascularity will be accurate regardless of lesion surface area. Accurate acquisition of this information is vital to clinical studies, as research has shown that lesion vascularity is as important as thickness in terms of prognosis, if not more so². All of these results show great promise, as clearly the probe's response to inhomogeneities is indicative of physical quantities of interest such as their size/depth and optical

properties. Through these phantom trials we have confirmed that we have the ability to probe tissue that will give us crucial information about both the type of lesion and its development. This is a significant step towards our goal of non-invasive diagnosis. New DOS technology holds great promise for detection of skin cancer, and this research is a vital step towards a means of fast and accurate diagnosis. It has the potential to revolutionize traditional methods and change the lives of millions of people who now or in the future will suffer from skin cancer.

ACKNOWLEDGEMENTS

This work was supported by: the Laser Microbeam and Medical Program (LAMMP) NIH grant P41 RR01192; the U.S. Air Force Office of Scientific Research, Medical Free-Electron Laser Program (F49620-00-2-0371 and FA9550-04-1-0101); The Beckman Foundation; the UC Irvine UROP Fellowship. The mention of commercial products, their sources, or their use in connection with material reported here is not to be construed as either an actual or implied endorsement of such products by the U.S. Food and Drug Administration.

REFERENCES

- [1] Buettner, P.G., et al., "Development of prognostic factors and survival in cutaneous melanoma over 25 years: An analysis of the Central Malignant Melanoma Registry of the German Dermatological Society," *Cancer*, 2005. **103**(3): p. 616-24.
- [2] Kashani-Sabet, M., et al., "Tumor vascularity in the prognostic assessment of primary cutaneous melanoma," *J Clin Oncol*, 2002. **20**(7): p. 1826-31.
- [3] Marghoob, A.A., et al., "Instruments and new technologies for the in vivo diagnosis of melanoma," *J Am Acad Dermatol*, 2003. **49**(5): p. 777-97; quiz 798-9.
- [4] Bevilacqua, F., et al., "Broadband absorption spectroscopy in turbid media by combined frequency-domain and steady-state methods," *Appl Opt*, 2000. **39**(34): p. 6498-507.
- [5] Swartling, J., J.S. Dam, and S. Andersson-Engels, "Comparison of spatially and temporally resolved diffuse-reflectance measurement systems for determination of biomedical optical properties," *Appl Opt*, 2003. **42**(22): p. 4612-20.
- [6] Fantini, S., et al., "Assessment of the size, position, and optical properties of breast tumors in vivo by noninvasive optical methods," *Appl Opt*, 1998. **37**(10): p. 1982-9.
- [7] Shah, N., et al., "Spatial variations in optical and physiological properties of healthy breast tissue," *J Biomed Opt*, 2004. **9**(3): p. 534-40.
- [8] Tseng, S.H., et al., "Determination of optical properties of superficial volumes of layered tissue phantoms," *IEEE Trans Biomed Eng*, 2008. **55**(1): p. 335-9.
- [9] Wang, L.V. and H. Wu, "Biomedical Optics: Principles and Imaging," 2007, Hoboken: John Wiley & Sons, Inc.
- [10] Backman, V., et al., "Detection of preinvasive cancer cells," *Nature*, 2000. **406**(6791): p. 35-6.
- [11] Kienle, A., et al., "Noninvasive Determination of the Optical Properties of Two-Layered Turbid Media," *Appl Opt*, 1998. **37**(4): p. 779-791.
- [12] Simpson, C.R., et al., "Near-infrared optical properties of ex vivo human skin and subcutaneous tissues measured using the Monte Carlo inversion technique," *Phys Med Biol*, 1998. **43**(9): p. 2465-78.
- [13] Tseng, S.H., A. Grant, and A.J. Durkin, "In vivo determination of skin near-infrared optical properties using diffuse optical spectroscopy," *J Biomed Opt*, 2008. **13**(1): p. 014016.
- [14] Durkin, A.J., S. Jaikumar, and R. Richards-Kortum, "Optically Dilute, Absorbing, and Turbid Phantoms For Fluorescence Spectroscopy of Homogeneous and Inhomogeneous Samples," *Appl. Spectrosc*, 1993. **47**(12): p. 2114-2121.
- [15] Pfefer, T.J., et al., "Modeling laser treatment of port wine stains with a computer-reconstructed biopsy," *Lasers Surg Med*, 1999. **24**(2): p. 151-66.
- [16] Streit, M. and M. Detmar, "Angiogenesis, lymphangiogenesis, and melanoma metastasis," *Oncogene*, 2003. **22**: p. 3172-9.
- [17] Prahl, S.A., "The adding-doubling method", in [Optical-Thermal Response of Laser Irradiated Tissue], A.J. Welch and M.J. van Gemert, Editors. 1995, Plenum Press: New York. p. 102-129.